inorganics

MDPI

Article

Magnetic and Thermoelectric Properties of Fe_2CoGa Heusler Compounds

Tetsuji Saito * and Hayai Watanabe

Graduate School of Engineering, Chiba Institute of Technology, Narashino 275-8588, Chiba, Japan
* Correspondence: tetsuji.saito@it-chiba.ac.jp

Abstract: The investigation of the properties of Heusler compounds is an important task that will pave the way for new applications in various fields related to magnetics and thermoelectrics. This study examines the magnetic and thermoelectric properties of Fe_2CoGa Heusler compounds prepared by casting and subsequent annealing. The Fe_2CoGa Heusler compound was found to be ferromagnetic, with a large saturation magnetization of 110 emu/g and a high Curie temperature of 1011 K. The Fe_2CoGa Heusler compound was a good thermoelectric material, with a negative Seebeck coefficient of −44 μV/K, a low electrical resistivity of 0.60 μΩm, and a high-power factor of 3000 $\mu W/mK^2$ at room temperature. The maximum power factor of 3230 $\mu W/mK^2$ for the Fe_2CoGa Heusler compound was obtained at 400 K. In order to improve the magnetic and thermoelectric properties of the Fe_2CoGa Heusler compound, $Fe_{2-x}Co_{1+x}Ga$ (x = 0–1) Heusler compounds were also prepared by casting and subsequent annealing. In the $Fe_{2-x}Co_{1+x}Ga$ (x = 0–1) Heusler compounds, the saturation magnetization slightly decreased, but the Curie temperature increased with increasing Co content (x). As regards the thermoelectric properties, the electrical resistivity of the $Fe_{2-x}Co_{1+x}Ga$ (x = 0.25–1) Heusler compounds was smaller than that of the Fe_2CoGa Heusler compound. The Seebeck coefficient and power factor of the $Fe_{1.75}Co_{1.25}Ga$ Heusler compound were more significant than those of the Fe_2CoGa Heusler compound. An increase in the Co content of the Fe_2CoGa Heusler compound did not improve the saturation magnetization but improved the Curie temperature and thermoelectric properties of the Fe_2CoGa Heusler compound. The $Fe_{1.75}Co_{1.25}Ga$ Heusler compound exhibited a high-power factor value of over 4000 $\mu W/mK^2$, which was comparable to that of the Bi_2Te_3 compound.

Keywords: iron alloys; Heusler compounds; thermoelectric properties; magnetic properties

check for updates

Academic Editor: Jean-François Halet

Received: 25 December 2024
Revised: 20 January 2025
Accepted: 21 January 2025
Published: 23 January 2025

Citation: Saito, T.; Watanabe, H. Magnetic and Thermoelectric Properties of Fe_2CoGa Heusler Compounds. *Inorganics* **2025**, *13*, 33. https://doi.org/10.3390/inorganics13020033

Copyright: © 2025 by the authors. Licensee MDPI, Basel, Switzerland. This article is an open access article distributed under the terms and conditions of the Creative Commons Attribution (CC BY) license (https://creativecommons.org/licenses/by/4.0/).

1. Introduction

Burning fossil fuels is still necessary to secure energy supplies, but this has a significant environmental impact; in particular, it can induce global warming. The growing concern over global warming makes it essential to reduce greenhouse gas emissions. Currently, we lose more than 60% of the energy generated from fuels worldwide, mainly in the form of waste heat [1]. To prevent the increase in global warming, it is essential to recover as much heat energy as possible and, thus, avoid wasted. However, many industries still fail to engage in waste heat utilization, since effective waste heat recovery systems have yet to be developed. As a result, various technologies for waste heat recovery are now being investigated, such as heat pipe systems, heat-to-power conversion systems, and thermoelectric systems [2–6]. Of these approaches, thermoelectric systems using thermoelectric materials are attracting increasing attention because they can directly convert

heat to electrical energy [1]. These systems are environmentally friendly, as they emit no pollutants, are highly reliable, and require minimal maintenance thanks to their lack of moving parts. The systems can be used over a wide temperature range, from the low-temperature waste heat of automobiles to the high-temperature waste heat of power plants and factories.

Thermoelectric materials exhibit the Seebeck effect, where heat is converted into electricity. It is well known that thermoelectric materials supply the electric power used in NASA's spacecraft, such as Voyager 1 and 2 [7]. Thermoelectric materials also exhibit the Peltier effect, by which electricity is converted into heat, namely the reverse of the Seebeck effect. Various cooling devices used with thermoelectric materials, such as thermoelectric coolers and devices used for the electric cooling of computers, are commercially available [8,9]. As regards thermoelectric materials, the energy conversion efficiency is usually evaluated by the dimensionless figure of merit ($ZT = (PF/\kappa)T$, where PF is the power factor ($PF = S^2\sigma$, where S is the Seebeck coefficient, σ is the electrical conductivity), κ is the thermal conductivity, and T is absolute temperature). A bismuth telluride (Bi_2Te_3) compound, which exhibits high PF and ZT values [10], has been employed as the thermoelectric material in thermoelectric devices [11–14]. However, the Bi_2Te_3 compound cannot be used for waste heat recovery because it contains the scarce and toxic element tellurium. New thermoelectric materials with nontoxic and abundant elements should be realized while increasing energy and environmental conservation awareness.

Since thermoelectric materials can directly convert waste heat into electricity, several materials, such as Pb-Te, Fe-Si, Mg-Si, skutterudite, and Heusler alloys, have been developed [15–19]. Fe-based alloys are the most promising candidates for waste heat recovery applications with respect to resource and environmental issues. The iron silicide (β-$FeSi_2$) compound is a typical Fe-based thermoelectric material [16]. Although the β-$FeSi_2$ compound exhibits a high S value, it has a small PF value due to its low electrical conductivity. As a result, there have been several efforts to improve the thermoelectric properties of the β-$FeSi_2$ compound for thermoelectric applications [20–26].

Another Fe-based thermoelectric material is the Fe-based Heusler compound. Heusler compounds have an ordered $L2_1$-type structure with the formula X_2YZ, in which X and Y are transition metals and Z is an element of the IIIA, IVA, or VA group on the periodic table [27–30]. The Heusler compounds were initially known as magnetic materials but have attracted much attention because of their potential for new applications, such as magnetic-field-induced shape memory materials [31,32]. Since the Fe_2VAl Heusler compound exhibits good thermoelectric properties, the Heusler compounds have attracted considerable attention as thermoelectric materials [33]. The thermoelectric properties of various Fe-based Heusler compounds, such as Fe_2CoAl, Fe_2TiAl, Fe_2TiSi, and Fe_2TiSn, have been studied [34–37]. Since the discovery that the Fe_2VAl Heusler compound exhibited semiconductor-like behavior as regards electrical resistivity, this compound has been intensively investigated as a thermoelectric material [33]. Although the ZT value of the Fe_2VAl Heusler compound is still smaller than that of the Bi_2Te_3 compound, the former exhibits a higher PF value, larger than the latter [38,39].

Another Fe-based Heusler compound, the Fe_2CoGa Heusler compound, is stable and has an $L2_1$ structure [40]. There have been several studies on the Fe_2CoGa Heusler compound [41–44], but they have mainly focused on the magnetic properties: the Fe_2CoGa Heusler compound displays a large saturation magnetization and a high Curie temperature. Recent work has shown that the Fe_2CoGa Heusler compound exhibits thermoelectric properties [44]. In this study, we investigate the thermoelectric properties of the Fe_2CoGa Heusler compound. Since the Fe_2CoGa Heusler compound is ferromagnetic, the substitution of Co for Fe in this compound will affect not only the magnetic properties, but

also the thermoelectric properties. Therefore, we discuss the magnetic and thermoelectric properties of the $Fe_{2+x}Co_{1-x}Ga$ (x = 0–1) Heusler compounds.

2. Results and Discussion

2.1. Fe_2CoGa Heusler Compound

First, we examined the structures of the Fe_2CoGa specimen. The XRD patterns of an as-cast Fe_2CoGa ingot and an annealed specimen are shown in Figure 1. The diffraction peaks in the XRD pattern of the as-cast Fe_2CoGa ingot were indexed to those of the Fe_2CoGa Heusler compound ($L2_1$ phase), but small unidentified peaks were also found in the XRD pattern. On the other hand, the diffraction peaks in the XRD pattern of the annealed specimen were well indexed to those of the Fe_2CoGa Heusler compound. This confirms that, if we are to obtain the Fe_2CoGa Heusler compound, we must anneal the as-case ingot for a long period at a high temperature. We investigated the magnetic and thermoelectric properties of the Fe_2CoGa Heusler compound.

Figure 2 shows the magnetization curve of the Fe_2CoGa Heusler compound. The specimen exhibited a high saturation magnetization (M_s) of 110 emu/g, which corresponds to 1.15 T in SI units. Thus, the saturation magnetization of the Fe_2CoGa Heusler compound (0.240 kg/mol) was calculated to be 4.76 μ_B. This obtained value of 4.76 μ_B was slightly smaller than the reported saturation magnetization values of 5.09–6.27 μ_B for a bulk specimen but comparable to those of 3.89–5.3 μ_B for nanoparticles [42–44].

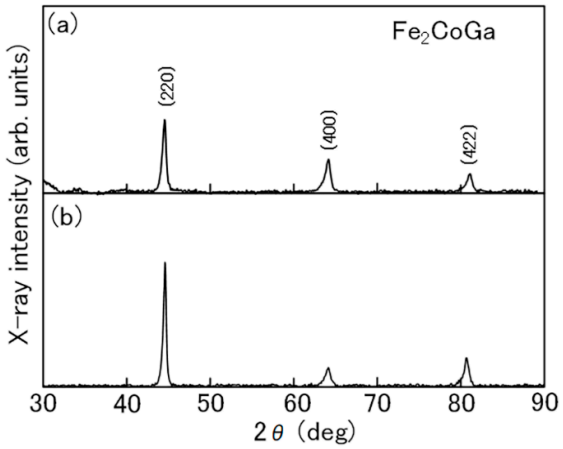

Figure 1. XRD patterns of (**a**) the as-cast Fe_2CoGa ingot and (**b**) the annealed specimen.

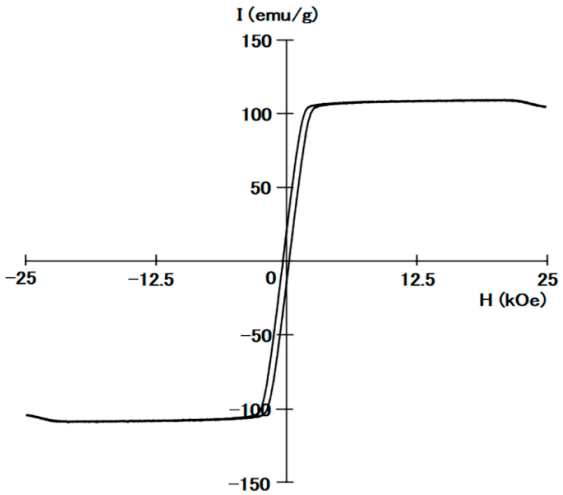

Figure 2. Magnetization curve of the Fe_2CoGa Heusler compound.

Since the Fe_2CoGa Heusler compound was found to be ferromagnetic, we examined its thermomagnetic curve. The result is shown in Figure 3. The thermomagnetic curve of the specimen exhibited a large magnetic transition at 1011 K. This magnetic transition is considered to be the Curie temperature (T_c) of the Fe_2CoGa Heusler compound. The obtained Curie temperature was smaller than the previously reported value of 1210 K for Fe_2CoGa nanoparticles [43] but agrees with the value shown in the Fe-Co-Ga phase diagram [45]. This confirms that the ferromagnetic Fe_2CoGa Heusler compound has a high Curie temperature.

According to the Fe-Co-Ga phase diagram, no Heusler compound ($L2_1$ phase) exists at a temperature of 1123 K. Therefore, we examined the stability of the Fe_2CoGa Heusler compound ($L2_1$ phase) using DTA. Figure 4 shows the DTA curve of the Fe_2CoGa Heusler compound. The specimen exhibited a small endothermic peak at around 1000 K (arrow #1) and a large endothermic peak at 1059 K (arrow #2). The first small endothermic peak was the magnetic transition. We were able to detect the magnetic transition, although we detected the Curie temperature more clearly in the thermomagnetic measurements (see Figure 3). The second large peak was the order–disorder phase transition from the ordered $L2_1$ phase to the disordered B2 phase. The observed order–disorder phase transition temperature was slightly higher than the reported value of 1043 K [41].

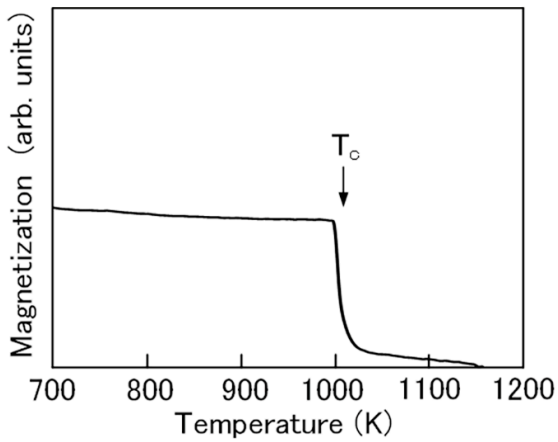

Figure 3. Thermomagnetic curves of the Fe_2CoGa Heusler compound.

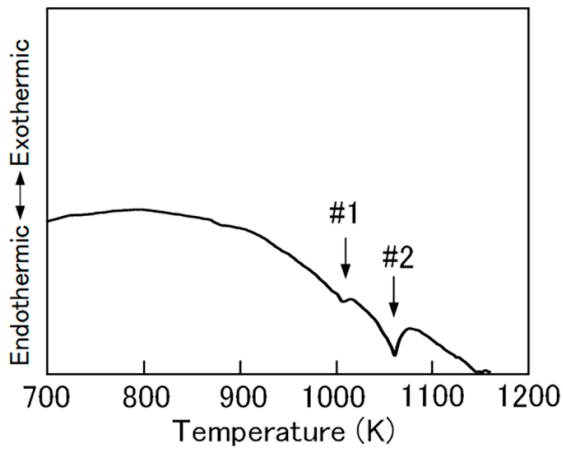

Figure 4. DTA curve of the Fe_2CoGa Heusler compound.

Next, we examined the thermoelectric properties of the Fe_2CoGa Heusler compound. Figure 5 shows the Seebeck coefficient (S) of the Fe_2CoGa Heusler compound as a function of the ambient temperature. The Fe_2CoGa specimen was found to be an n-type thermoelectric material characterized by a negative Seebeck coefficient. The Seebeck coefficient was

−44 μV/K at room temperature. The Seebeck coefficient of the specimen increased with increasing temperature. The maximum Seebeck coefficient of −48 μV/K was achieved in the Fe_2CoGa Heusler compound when measured at an ambient temperature of 600 K. Thus, the Fe_2CoGa Heusler compound can be considered a candidate as a thermoelectric material. A further increase in the ambient temperature did not increase the Seebeck coefficient. Therefore, in this experiment, we examined the thermoelectric properties of the Fe_2CoGa Heusler compound up to an ambient temperature of 600 K.

Another essential property of a thermoelectric material is its electrical conductivity. In this experiment, we examined electrical resistivity (resistivity is the inverse of conductivity). The result is shown in Figure 6. The Fe_2CoGa Heusler compound exhibited a low electrical resistivity in the temperature range investigated in this study, with a value of 0.60 μΩm at room temperature. Therefore, the electrical resistivity of the Fe_2CoGa Heusler compound is sufficiently small for these compounds to be thermoelectric materials.

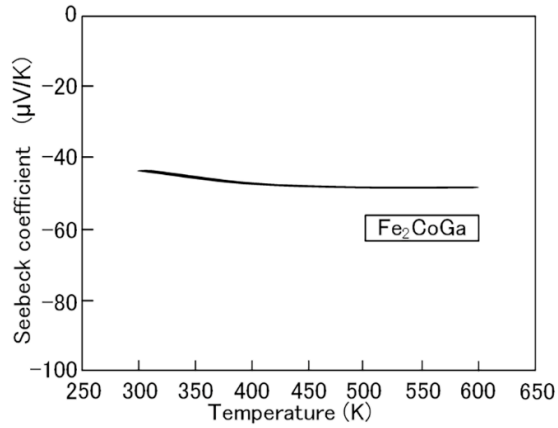

Figure 5. Seebeck coefficient as a function of the ambient temperature for the Fe_2CoGa Heusler compound.

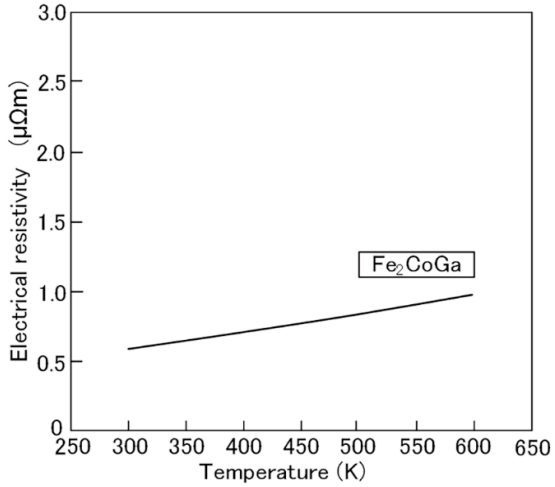

Figure 6. Electrical resistivity as a function of the ambient temperature for the Fe_2CoGa Heusler compound.

To evaluate the thermoelectric properties of the Fe_2CoGa Heusler compound, we calculated the power factor ($PF = S^2/\rho$). Figure 7 shows the power factor (PF) of the Fe_2CoGa Heusler compound. The power factor of the specimen increased from 3000 μW/mK^2 at room temperature to 3200 μW/mK^2 at 400 K and then decreased with increasing ambient temperature. We found that the Fe_2CoGa Heusler compound exhibited a high-power factor. The achieved power factor of the Fe_2CoGa Heusler compound was almost the same as that

of the Fe_2VAl Heusler compound, but the power factor was lower than that of the Bi_2Te_3 compound [39].

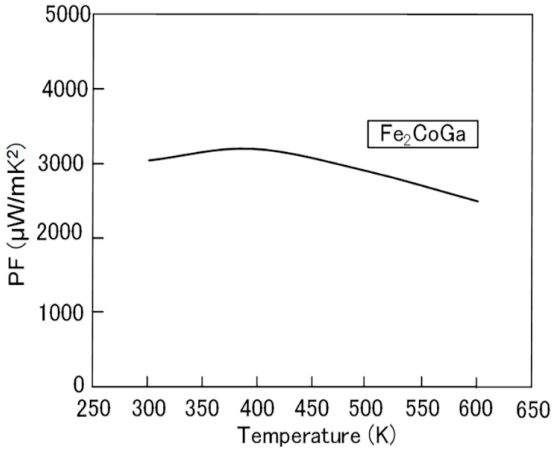

Figure 7. Power factor as a function of ambient temperature for the Fe_2CoGa Heusler compound.

2.2. $Fe_{2-x}Co_{1+x}Ga$ (x = 0–1) Heusler Compounds

It is known that the Seebeck coefficient of the Fe_2VAl Heusler compound can be improved by substituting Co for Fe [45,46]. In the Fe_2VAl Heusler compound, the shift of the Fermi level by doping or off-stoichiometry causes an enhancement in the Seebeck coefficient. As with the Fe_2VAl Heusler compound, the thermoelectric properties of the Fe_2CoGa Heusler compound might be improved by substituting Co for Fe. Therefore, we prepared $Fe_{2-x}Co_{1+x}Ga$ (x = 0–1) Heusler compounds and investigated their magnetic and thermoelectric properties.

The structures of the $Fe_{2-x}Co_{1+x}Ga$ (x = 0–1) annealed specimen were found to be the Heusler compound ($L2_1$ phase). The isothermal section at 973 K for the Fe-Co-Ga phase diagram is shown in Figure 8. According to the Fe-Co-Ga phase diagram shown in Figure 8, the equilibrium phase in the $Fe_{2-x}Co_{1+x}Ga$ (x = 0–1) annealed specimens is the Heusler compound ($L2_1$ phase) at 973 K. Thus, $Fe_{2-x}Co_{1+x}Ga$ (x = 0–1) Heusler compounds were obtained by annealing the as-cast ingots (see Figure 9). We investigated the magnetic and thermoelectric properties of these compounds.

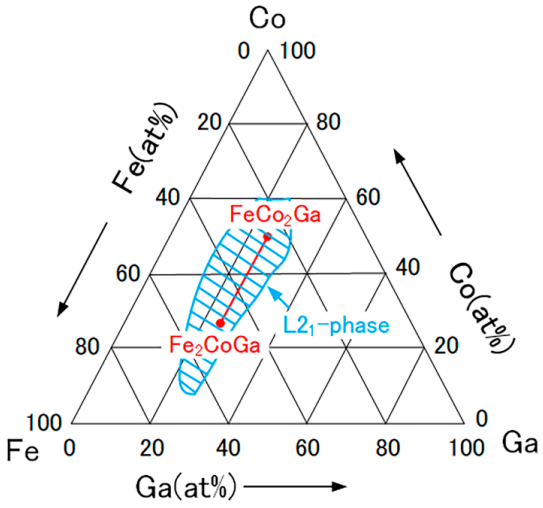

Figure 8. Fe-Co-Ga phase diagram with the composition of $Fe_{2-x}Co_{1+x}Ga$ (x = 0–1) [47].

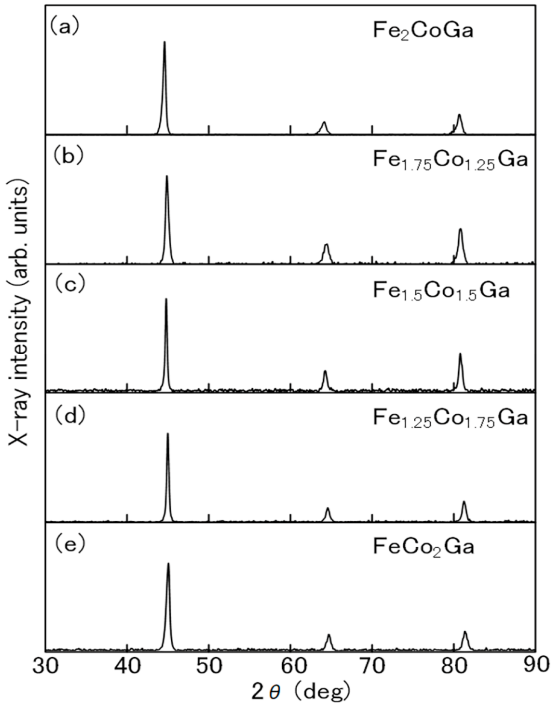

Figure 9. XRD patterns of the $Fe_{2-x}Co_{1+x}Ga$ (x = 0–1) Heusler compounds.

We examined the magnetization curves of the $Fe_{2-x}Co_{1+x}Ga$ (x = 0–1) Heusler compounds, and we plot the saturation magnetization values that we obtained in Figure 10. The saturation magnetization of the $Fe_{2-x}Co_{1+x}Ga$ (x = 0–1) specimens decreased slightly from 110 emu/g to 106 emu/g as the Co content increased. Although cobalt's saturation magnetization is lower than iron's, Fe-Co alloys have a higher saturation magnetization than Fe [48,49]. Thus, substituting Co for Fe in Fe-based alloys such as Nd-Fe-B magnets results in an increase in the saturation magnetization [50]. However, the substitution of Co for Fe in the $FeCo_2Ga$ Heusler compound resulted in a decrease in the saturation magnetization.

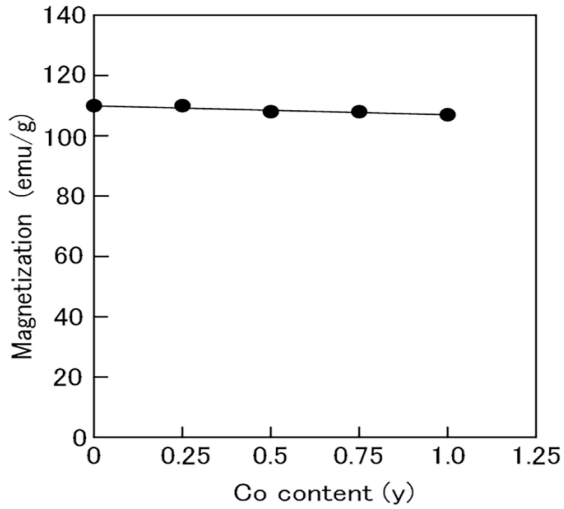

Figure 10. Saturation magnetization of the $Fe_{2-x}Co_{1+x}Ga$ (x = 0–1) Heusler compounds.

We examined the thermomagnetic curves of the $Fe_{2-x}Co_{1+x}Ga$ (x = 0–1) Heusler compounds, and the Curie temperature values that we obtained are summarized in Figure 11. The Curie temperature of the $Fe_{2-x}Co_{1+x}Ga$ (x = 0–1) Heusler compounds increased with the Co content. Unlike the case of the saturation magnetization, the substitution of Co for Fe in the Fe_2CoGa Heusler compound increased its Curie temperature from 1011 K for

the Fe_2CoGa Heusler compound to 1109 K for the $FeCo_2Ga$ Heusler compound. Cobalt is known as the only alloying element that substantially increases the Curie temperature of iron [49]. For example, the substitution of Co for Fe in Nd-Fe-B magnets increases their Curie temperature [50]. It was found that the substitution of Co for Fe in the $FeCo_2Ga$ Heusler compound also resulted in an increase in the Curie temperature.

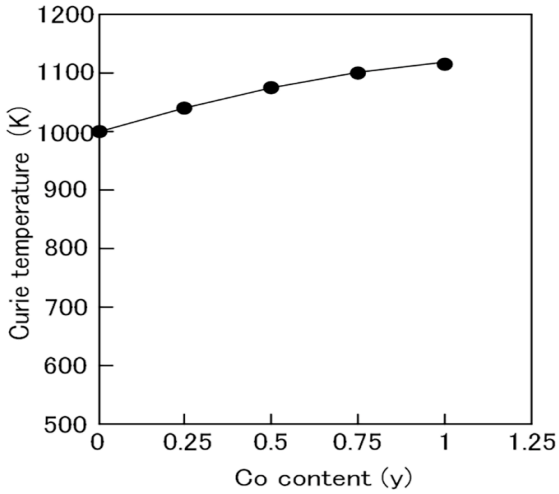

Figure 11. Curie temperatures of the Fe2-xCo1+xGa (x = 0–1) Heusler compounds.

The Seebeck coefficient of the $Fe_{2-x}Co_{1+x}Ga$ (x = 0–1) Heusler compounds is shown in Figure 12. The substitution of Co for Fe in the Fe_2CoGa Heusler compound did not change the nature of the thermoelectric material; that is to say, $Fe_{2-x}Co_{1+x}Ga$ (x = 0–1) Heusler compounds are n-type thermoelectric materials. However, the Co substitution significantly affects the Seebeck coefficient value. Regardless of the ambient temperature, a small Co substitution resulted in an increase in the Seebeck coefficient, but a large Co substitution resulted in a decrease in the Seebeck coefficient. The maximum Seebeck coefficient of −52 μV/K was achieved in the $Fe_{1.75}Co_{1.25}Ga$ Heusler compound when measured at an ambient temperature of 600 K. This indicates that the Co substitution can improve the Seebeck coefficient of the Fe_2CoGa Heusler compound as with the Fe_2VAl Heusler compound.

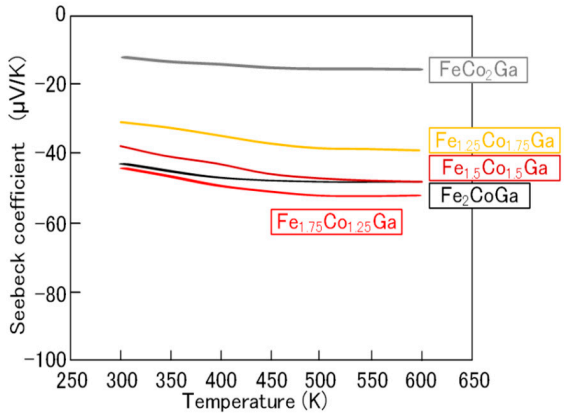

Figure 12. Seebeck coefficient as a function of the ambient temperature for the Fe2-xCo1+xGa (x = 0–1) Heusler compound.

The electrical resistivity of the $Fe_{2-x}Co_{1+x}Ga$ (x = 0–1) Heusler compounds is shown in Figure 13. Regardless of the ambient temperature, the electrical resistivity of the $Fe_{2-x}Co_{1+x}Ga$ (x = 0–1) Heusler compounds decreased with increasing Co content. The

Fe_2CoGa Heusler compound had a low electrical resistivity of 0.60 μΩm at room temperature, but the $FeCo_2Ga$ Heusler compound exhibited a lower electrical resistivity of 0.20 μΩm at room temperature. This indicates that the Co substitution can also improve the electrical resistivity of the Fe_2CoGa Heusler compound.

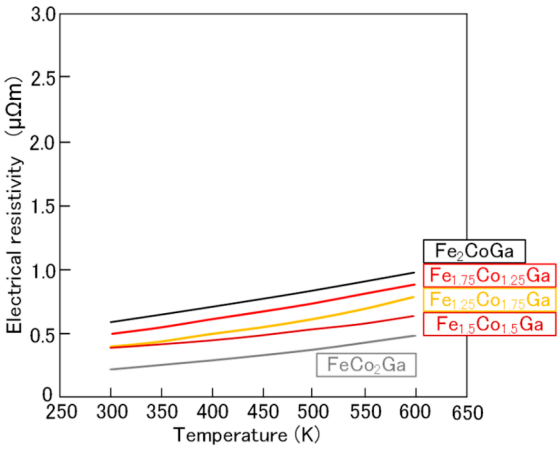

Figure 13. Electrical resistivity as a function of the ambient temperature for the Fe2-xCo1+xGa (x = 0–1) Heusler compound.

Finally, the power factors (PF) of the $Fe_{2-x}Co_{1+x}Ga$ (x = 0–1) Heusler compounds are shown in Figure 14. In the power factor ($PF = S^2/\rho$), the effect of the Seebeck coefficient (S) is stronger than that of the electrical resistivity (ρ). In this experiment, the maximum Seebeck coefficient was achieved in the $Fe_{1.75}Co_{1.25}Ga$ Heusler compound, so the maximum power factor was also achieved in the $Fe_{1.75}Co_{1.25}Ga$ Heusler compound. The power factor of the $Fe_{1.75}Co_{1.25}Ga$ Heusler compound increased from 4000 $\mu W/mK^2$ at room temperature to 4270 $\mu W/mK^2$ at 400 K and then decreased as the ambient temperature increased. This confirms that the Co substitution can improve the thermoelectric properties of the Fe_2CoGa Heusler compound. The achieved power factor of the Fe_2CoGa Heusler compound was almost the same as that of the Bi_2Te_3 compound (PF = 3800 $\mu W/mK^2$ at 320 K) [39]. However, this value is not yet comparable to that of the Ta-doped Fe_2VAl compound (PF = 6500 $\mu W/mK^2$ at 340 K) [40]. The power factor of the Fe_2CoGa Heusler compound would be further improved by doping other elements.

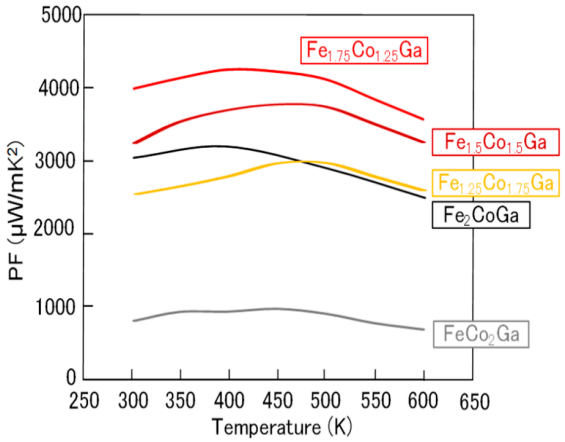

Figure 14. Power factors (PF) as a function of the ambient temperature for the Fe2-xCo1+xGa (x = 0–1) Heusler compound.

3. Materials and Methods

3.1. Sample Preparation

Fe-Co-Ga alloys with a nominal composition of Fe_2CoGa were prepared from Fe (99.9%), Co (99.9%), and Ga (99.9%) metals. The metal mixtures were induction-melted and then cast into a Cr-coated copper mold in an argon atmosphere. The as-cast ingots were cylindrical, 3 mm in diameter, and 30–50 mm long. The ingots were wrapped in tantalum foil and then annealed in an argon atmosphere at 1073 K for 20 h to stabilize them and obtain a Heusler structure. Fe-Co-Ga alloys with a nominal composition of $Fe_{2+x}Co_{1-x}Ga$ (x = 0–1) were also prepared under the same conditions.

3.2. Characterization

For the property measurements, disc-shaped specimens (0.5 mm thickness and 3 mm in diameter) and cylindrical specimens (8 mm thickness and 3 mm in diameter) were cut from the cast ingots. The phases of the specimens were characterized by X-ray diffraction (XRD) using Cu Kα radiation (MiniFlex600, Rigaku, Tokyo, Japan) and differential thermal analysis (DTA) in an argon atmosphere at a heating rate of 0.16 K/s (STA7300, Hitachi High-tech, Tokyo, Japan). The magnetic properties of the specimens were characterized using a vibrating sample magnetometer (VSM) with an applied magnetic field of 25 kOe (BHV-525RSCM, Riken Denshi, Tokyo, Japan). Disc-shaped specimens were measured parallel to the disc surface in the hysteresis measurements to avoid the need for demagnetization correction. Thermomagnetic curves for the specimens were obtained using DTA equipped with a permanent magnet. The thermoelectric properties of the specimens were characterized using a Seebeck coefficient/electric resistance measurement system (ZEM-3M8, Advance Riko, Yokohama, Japan). The Seebeck coefficient (S) of the cylindrical specimens was determined by measuring the upper and lower temperatures with thermocouples, and the electric resistance (ρ) was measured with the standard DC four-terminal method in a low-pressure helium atmosphere. The thermoelectric measurements are detailed in Ref. [34]. The power factors (PF) of the specimens were determined using the equation $PF = S^2/\rho$, where S is the Seebeck coefficient and ρ is the electrical resistance (ρ) value.

4. Conclusions

The Fe_2CoGa Heusler compound was found to be ferromagnetic, with a large saturation magnetization (M_s) of 110 emu/g and a high Curie temperature (T_c) of 1011 K. It was found that the Fe_2CoGa Heusler compound is a good thermoelectric material, with a Seebeck coefficient (S) of -44 μV/K and a high power factor (PF) of 3000 $\mu W/mK^2$ at room temperature. The magnetic and thermoelectric properties of the Fe_2CoGa Heusler compound were improved by substituting Co for Fe in the Fe_2CoGa Heusler compound. The Co substitution did not increase the saturation magnetization but led to an increase in the Curie temperature. Regarding the thermoelectric properties, a small Co substitution greatly improved the thermoelectric properties, but a large Co substitution decreased the thermoelectric properties. The $Fe_{1.75}Co_{1.25}Ga$ Heusler compound exhibited a high-power factor (PF) value of over 4000 $\mu W/mK^2$ at room temperature, comparable to that of the Bi_2Te_3 compound.

Author Contributions: T.S.: methodology, writing, formal analysis, original draft preparation; H.W.: methodology, investigation, formal analysis. All authors have read and agreed to the published version of the manuscript.

Funding: This research received no external funding.

Data Availability Statement: Data are contained within the article.

Acknowledgments: The technical support of K. Ito is acknowledged.

Conflicts of Interest: The authors declare no conflicts of interest.

References

1. Zhang, X.; Zhao, L.D. Thermoelectric materials: Energy conversion between heat and electricity. *J. Materiomics* **2015**, *1*, 92–105. [CrossRef]
2. Jouhara, H.; Olabi, A.G. Editorial: Industrial waste heat recovery. *Energy* **2018**, *160*, 1–2. [CrossRef]
3. Brückner, S.; Liu, S.; Miró, L.; Radspieler, M.; Cabeza, L.F.; Lävemann, E. ndustrial waste heat recovery technologies: An economic analysis of heat transformation technologies. *Appl. Energy* **2015**, *151*, 157–167. [CrossRef]
4. Law, R.; Harvey, A.; Reay, D. A knowledge-based system for low-grade waste heat recovery in the process industries. *Appl. Therm. Eng.* **2016**, *94*, 590–599. [CrossRef]
5. Huang, F.; Zheng, J.; Baleynaud, J.M.; Lu, J. Heat recovery potentials and technologies in industrial zones. *J. Energy Inst.* **2017**, *90*, 951–961. [CrossRef]
6. Jouhara, H.; Khordehgah, N.; Almahmoud, S.; Delpech, B.; Chauhan, A.; Tassou, S.A. Waste Heat Recovery Technologies and Applications. *Therm. Sci. Eng. Prog.* **2018**, *6*, 268–289. [CrossRef]
7. Thermoelectric Devices Cool, Power Electrics. Available online: https://spinoff.nasa.gov/Spinoff2009/ip_4.html (accessed on 20 December 2024).
8. Savage, N. Thermoelectric coolers. *Nat. Photonics* **2009**, *3*, 541–542. [CrossRef]
9. Al-Shehria, S.; Saberb, H.H. Experimental investigation of using thermoelectric cooling for computer chips. *J. King Saud Univ.–Eng. Sci.* **2019**, *32*, 321–329. [CrossRef]
10. Goldsmid, H.J. Bismuth Telluride and Its Alloys as Materials for Thermoelectric Generation. *Materials* **2014**, *7*, 2577–2592. [CrossRef]
11. Satterthwaite, C.B.; Ure, R.W., Jr. Electrical and Thermal Properties of Bi2Te3. *Phys. Rev.* **1957**, *108*, 1164–1170. [CrossRef]
12. Rosi, F.D.; Abeles, B.; Jensen, R.V. Materials for thermoelectric refrigeration. *J. Phys. Chem. Solids* **1959**, *10*, 191–200. [CrossRef]
13. Wada, H.; Sato, T.; Takahashi, K.; Nakatsukasa, K. The anisotropic powder metallurgy of *n*-type $Bi_2Te_{2.85}Se_{0.15}$ thermoelectric material. *J. Mater. Res.* **1990**, *5*, 1052–1057. [CrossRef]
14. Mamur, H.; Bhuiyan, M.R.A.; Korkmaz, F.; Nil, M. A review on bismuth telluride (Bi_2Te_3) nanostructure for thermoelectric applications. *Renew. Sust. Energy Rev.* **2018**, *82*, 4159–4169. [CrossRef]
15. Gomez, M.P.; Stevenson, D.A.; Huggins, R.A. Self-diffusion of Pb and Te in lead telluride. *J. Phys. Chem. Solids* **1971**, *32*, 335–344. [CrossRef]
16. Ware, R.M.; McNeill, D.J. Iron disilicade as a thermoelectric generator material. *Proc. Inst. Electr. Eng.* **1964**, *111*, 178–182. [CrossRef]
17. Zaitsev, V.K.; Fedorov, M.I.; Gurieva, E.A.; Eremin, I.S.; Konstantinov, P.P.; Samunin, A.Y.; Vedernikov, M.V. Highly effective $Mg_2Si_{1-x}Sn_x$ thermoelectrics. *Phys. Rev. B* **2006**, *74*, 045207. [CrossRef]
18. Rogl, G.; Rogl, P. Skutterudites, a most promising group of thermoelectric materials. *Curr. Opin. Green Sustainable Chem.* **2017**, *4*, 50–57. [CrossRef]
19. Hanada, Y.; Suzuki, R.O.; Ono, K. Seebeck coefficient of (Fe,V) Al alloys. *J. Alloys Compd.* **2001**, *329*, 63–68. [CrossRef]
20. Birkholz, U.; Schelm, J. Electrical Investigation of the Semiconductor-to-Metal Transition in $FeSi_2$. *Phys. Stat. Sol. B* **1969**, *34*, K177–K180. [CrossRef]
21. Nishida, I. Study of Semiconductor-to-Metal Transition in Mn-Doped $FeSi_2$. *Phys. Rev. B* **1973**, *7*, 2710–2713. [CrossRef]
22. Piton, J.P.; Fay, M.F. Phase changes in iron–silicon alloys around the composition $FeSi_2$. *Acad. C. R. Sci.* **1968**, *C266*, 514–516.
23. Kojima, T. Semiconducting and Thermoelectric Properties of Sintered Iron Disilicide. *Phys. Stat. Sol. A* **1989**, *111*, 233–242. [CrossRef]
24. Ohta, Y.; Miura, S.; Mishima, Y. Thermoelectric semiconductor iron disilicides produced by sintering elemental powders. *Intermetallics* **1999**, *7*, 1203–1210. [CrossRef]
25. Dąbrowski, F.; Ciupiński, Ł.; Zdunek, J.; Kruszewski, J.; Zybała, R.; Michalski, A.; Kurzydłowski, K.J. Microstructure and thermoelectric properties of p and n type doped β-$FeSi_2$ fabricated by mechanical alloying and pulse plasma sintering. *Mater. Today Proc.* **2019**, *8*, 531–539. [CrossRef]
26. Saito, T.; Asakawa, R. Production of (Fe,Co)Si_2 and (Fe.Mn)Si_2 thermoelectric materials by spark plasma sintering. *Crystals* **2023**, *14*, 56. [CrossRef]
27. Buschow, K.H.J.; van Engen, P.G. Magnetic and magneto-optical properties of heusler alloys based on aluminum and gallium. *J. Magn. Magn. Mater.* **1981**, *25*, 90–96. [CrossRef]
28. Tuszýnski, M.; Zarek, W.; Popiel, E.S. Magnetic properties of atomically disordered $Fe_{3-x}V_xAl$ alloys with $x \leqq 0$. *Hyperfine Interact.* **1990**, *59*, 369–372. [CrossRef]

29. Graf, T.; Felser, C.; Parkin, S.S.P. Simple rules for the understanding of Heusler compounds. *Prog. Solid State Chem.* **2011**, *39*, 1–50. [CrossRef]
30. Palmstrøm, C.J. Heusler compounds and spintronics. *Prog. Cryst. Growth Charact. Mater.* **2016**, *62*, 371–397. [CrossRef]
31. Ullakko, K.; Huang, J.K.; Kantner, C.; O'Handley, R.C. Large magnetic-field-induced strains in Ni_2MnGa single crystals. *Appl. Phys. Lett.* **1996**, *69*, 1966–1968. [CrossRef]
32. Kainuma, R.; Imano, Y.; Ito, W.; Sutou, Y.; Morito, H.; Okamoto, S.; Kitakami, O.; Oikawa, K.; Fujita, A.; Kanomata, T.; et al. Magnetic-field-induced shape recovery by reverse phase transformation. *Nature* **2006**, *439*, 957–960. [CrossRef]
33. Nishino, Y.; Kato, M.; Asano, S.; Soda, K.; Hayasaki, M.; Miuztani, U. Semiconductorlike Behavior of Electrical Resistivity in Heusler-type Fe_2VAl Compound. *Phys. Rev. Lett.* **1997**, *79*, 1909. [CrossRef]
34. Saito, T.; Hamane, D.N. Magnetic and thermoelectric properties of melt-spun ribbons of Fe_2XAl (X = Co, Ni) Heusler compounds. *J. Appl. Phys.* **2018**, *124*, 075105. [CrossRef]
35. Suzuki, R.O.; Kyono, T. Thermoelectric properties of Fe_2TiAl Heusler alloys. *J. Alloys Compd.* **2004**, *377*, 38–42. [CrossRef]
36. Yabuuchi, S.; Okamoto, M.; Nishide, A.; Kurosaki, Y.; Hayakawa, J. Large Seebeck coefficients of Fe_2TiSn and Fe_2TiSi: Fisrt-Principles study. *Appl. Phys. Express* **2013**, *6*, 022504. [CrossRef]
37. Saito, T.; Kamishima, S. Magnetic and thermoelectric properties of Fe-Ti-Sn Heusler alloys. *IEEE Trans. Magn.* **2019**, *55*, 2900104. [CrossRef]
38. Renard, K.; Mori, A.; Yamada, Y.; Tanaka, S.; Miyazaki, H.; Nishino, Y. Thermoelectric properties of the Heusler-type $Fe_2VTa_xAl_{1-x}$. *J. Appl. Phys.* **2014**, *115*, 033707. [CrossRef]
39. Zhang, Z.; Cao, Y.; Tao, Q.; Yan, Y.; Su, X.; Tang, X. Distinct role of Sn and Ge doping on thermoelectric properties in p-type $(Bi, Sb)_2Te_3$-alloys. *J. Solid State Chem.* **2020**, *292*, 121722. [CrossRef]
40. Jaggi, N.K.; Rao, K.R.P.M.; Grover, A.K.; Gupta, L.C.; Vijayaraghanvan, R.; Khoi, L.D. Mössbauer and NMR study of site preference and local environment effects in Co_2FeGa & Fe_2CoGa. *Hyperfine Interact* **1978**, *4*, 402–406.
41. Ducher, R.; Kainuma, R.; Ohnuma, I.; Ishida, K. Phase equilibria and stability of B2 and $L2_1$ ordered phases in the Co-Fe-Ga Hequsler alloy system. *J. Alloys Compd.* **2007**, *437*, 93–101. [CrossRef]
42. Wang, C.; Gasper, F.; Gasi, T.; Ksenofontov, V.; Balke, B.; Fecher, G.H.; Felser, C.; Hwu, Y.K.; Lee, J.J. Structural and magnetic properties of Fe_2CoGa Heusler nanoparticles. *J. Phys. D Appl. Phys.* **2012**, *45*, 295001. [CrossRef]
43. Srivastave, M.; Sahariah, M.B.; Srinivasan, A. Size-dependent properties of single domain Fe_2CoGa nanoparticles prepared by a facile template-less chemical route. *J. Mater. Chem. C* **2022**, *10*, 11946–11958. [CrossRef]
44. Mende, F.; Noky, J.; Guin, S.N.; Fecher, G.H.; Manna, K.; Adler, P.; Schnelle, W.; Sun, Y.; Fu, C.; Felser, C. Large anomalous Hall and Nernst effects in high curie temperature iron-based Heusler compounds. *Adv. Sci.* **2021**, *2*, 100782. [CrossRef]
45. Nakayama, H.; Ide, N.; Nishino, Y. Thermoelectric Properties of P-Type Heusler Compounds $(Fe_{2-x}Co_x)(V_{1-y}Ti_y)Al$. *Mater. Trans.* **2008**, *49*, 1858–1862. [CrossRef]
46. Lu, W.; Zhang, W.; Chen, L. Thermoelectric properties of $(Fe_{1-x}Co_x)_2VAl$ Heusler-type compounds. *J. Alloys Compd.* **2009**, *484*, 812–815. [CrossRef]
47. Raghavan, V. Co-Fe-Ga(Cobalt-Iron-Gallium). *J. Phase Equilibria Diffus.* **2008**, *29*, 438–439. [CrossRef]
48. Chikazumi, S.; Charap, S.H. *Physics of Magnetism*; John Wiley & Sons, Inc.: Hoboken, NJ, USA, 1964; pp. 72–73.
49. Cullity, B.D.; Graham, C.D. *Introduction to Magnetic Materials*; John Wiley & Sons, Inc.: Hoboken, NJ, USA, 2008; p. 466.
50. Shibata, T.; Arai, S. Magnetic properties and crystal structures of Nd-Fe-Co-B system permanent magnets. *IEEE Trans. Magn.* **1985**, *TJMJ-1*, 420–425. [CrossRef]

Disclaimer/Publisher's Note: The statements, opinions and data contained in all publications are solely those of the individual author(s) and contributor(s) and not of MDPI and/or the editor(s). MDPI and/or the editor(s) disclaim responsibility for any injury to people or property resulting from any ideas, methods, instructions or products referred to in the content.